1 Ubiquitous production of branched glycerol dialkyl glycerol tetraethers (brGDGTs) in

2 global marine environments: a new source indicator for brGDGTs

3 Wenjie Xiao[1,2], Yinghui Wang[2], Shangzhe Zhou[2], Limin Hu[3], Huan Yang[4], Yunping Xu[1,2*]

4 [1]Shanghai Engineering Research Center of Hadal Science and Technology, College of Marine
5 Sciences, Shanghai Ocean University, Shanghai 201306, China
6 [2]MOE Key Laboratory for Earth Surface Process, College of Urban and Environmental Sciences,
7 Peking University, Beijing 100871, China
8 [3]Key Laboratory of Marine Sedimentology and Environmental Geology, First Institute of
9 Oceanography, State Oceanic Administration, Qingdao 266061, China
10 [4]State Key Laboratory of Biogeology and Environmental Geology, China University of Geosciences,
11 Wuhan 430074, China
12 Corresponding author: Y Xu (ypxu@shou.edu.cn)

13

14 Abstract. Presumed source specificity of branched glycerol dialkyl glycerol tetraethers

15 (brGDGTs) from bacteria thriving in soil/peat and isoprenoid GDGTs (iGDGTs) from

16 aquatic organisms led to the development of several biomarker proxies for

17 biogeochemical cycle and paleoenvironmental reconstructions. However, recent studies

18 reveal that brGDGTs are also produced in aquatic environments besides soils and peat.

19 Here we examined three cores from the Bohai Sea and found distinct difference in

20 brGDGT compositions varying with the distance from the Yellow River mouth. We thus

21 propose an abundance ratio of hexamethylated to pentamethylated brGDGT (IIIa/IIa)

22 to evaluate brGDGT sources. The compilation of globally distributed 1354 marine

23 sediments and 589 soils shows that the IIIa/IIa ratio is generally <0.59 in soils, 0.59–

24 0.92 and >0.92 in marine sediments with and without significant terrestrial inputs,

25 respectively. Such disparity confirms the existence of two sources for brGDGTs, a

26 terrestrial origin with lower IIIa/IIa and a marine origin with higher IIIa/IIa, which is

27 likely attributed to generally higher pH and the production of brGDGTs in cold deep

28 water in marine waters. The application of the IIIa/IIa ratio to the East Siberian Arctic

29 Shelf proves it a sensitive source indicator for brGDGTs, which is helpful for accurate

30 estimation of organic carbon source and paleoclimates in marine settings.

31

32 1 Introduction

33   Glycerol dialkyl glycerol tetraethers (GDGTs), membrane lipids of archaea and

34 certain bacteria, are widely distributed in marine and terrestrial environments (Schouten

35 et al., 2013). These lipids have been a focus of attention of organic geochemists for

36 more than ten years because they can be used to estimate environmental variables in

37 the past such as temperature, soil pH, organic carbon source and microbial community

38 structure (e.g., Schouten et al., 2002; Hopmans et al., 2004; Weijers et al., 2006; Lipp

39 et al., 2008; Kim et al., 2010; Peterse et al., 2012; Zhu et al., 2016). There are generally

40 two types of GDGTs, isoprenoid (iGDGTs) and non-isoprenoid, branched GDGTs

41 (brGDGTs; Fig. 1). The former group is more abundant in aquatic settings and generally

42 thought to be produced by Thaumarchaeota, a specific genetic cluster of the archaea

43 domain (Sinninghe Damsté et al., 2002; Schouten et al., 2008), although Euryarchaeota

44 may be a significant source of iGDGTs in the ocean (e.g., Lincoln et al., 2014). In

45 contrast, the 1,2-di-O-alkyl-sn-glycerol configuration of brGDGTs was interpreted as

46 evidence for a bacterial rather than archaeal origin for brGDGTs (Sinninghe Damsté et

47 al., 2000; Weijers et al., 2006). So far, only one brGDGT with two 13,16-dimethyl

48 octacosanyl moieties was unambiguously detected in two species of Acidobacteria

49 (Sinninghe Damsté et al., 2011), which hardly explains high diversity and ubiquitous

50 occurrence of up to 15 brGDGT isomers in environments (Weijers et al., 2007b; De

51 Jonge et al., 2014). Therefore, other biological sources of brGDGTs, although not yet

52 identified, are likely.

53   The source difference between brGDGTs and iGDGTs led researchers to

54 developing a branched and isoprenoid tetraether (BIT) index, expressed as relative

55 abundance of terrestrial-derived brGDGTs to aquatic-derived Thaumarchaeotal

56 (Hopmans et al., 2004). Subsequent studies found that the BIT index is specific for soil

organic carbon because GDGTs are absent in vegetation (e.g., Walsh et al., 2008; Sparkes et al., 2015). The BIT index is generally higher than 0.9 in soils, but close to 0 in marine sediments devoid of terrestrial inputs (Weijers et al., 2006; Weijers et al., 2014). Since its advent, the BIT index has been increasingly used to trace soil organic matter in different environments (e.g., Herfort et al., 2006; Kim et al., 2006; Blaga et al., 2011; Loomis et al., 2011; Wu et al., 2013). However, the BIT index is not just dependent on the abundance of brGDGTs, which reflects the input of soil organic matter, but also on the abundance of crenarchaeol, which is linked to marine productivity (e.g., Herfort et al., 2006；Smith et al, 2010; Fietz et al., 2011). Besides the BIT index, Weijers et al. (2007b) found that the number of cyclopentane moieties of brGDGTs, expressed as Cyclization of Branched Tetraethers (CBT), correlated negatively with soil pH, while the number of methyl branches of brGDGTs, expressed as Methylation of Branched Tetraethers (MBT), was dependent on annual mean air temperature (MAT) and to a lesser extent on soil pH. The MBT/CBT proxies were further corroborated by subsequent studies (e.g., Sinninghe Damsté et al., 2008; Peterse et al., 2012; Yang et al., 2014a). Assuming that brGDGTs preserved in marine sediments close to the Congo River outflow were derived from soils in the river catchment, Weijers et al. (2007a) reconstructed large-scale continental temperature changes in tropical Africa that span the past 25,000 years by using the MBT/CBT proxy. Recently, De Jonge et al. (2013) used tandem high performance liquid chromatography-mass spectrometry (2D HPLC-MS) and identified a series of novel 6-methyl brGDGTs which were previously coeluted with 5-methyl brGDGTs. This finding resulted in the redefinition and recalibration of brGDGTs' indices (e.g., De Jonge et al., 2014; Xiao et al., 2015).

One underlying assumption of all brGDGT-based parameters is their source specificity, i.e., brGDGTs are only biosynthesized by bacteria thriving in soils and peat. Several studies, however, observed different brGDGT compositions between marine sediments and soils on adjacent lands, supporting in situ production of brGDGTs in marine environments (e.g., Peterse et al., 2009a; Zhu et al., 2011; Liu et al., 2014; Weijers et al., 2014; Zell et al., 2014), analogous to lacustrine settings (e.g., Sinninghe Damsté et al., 2009; Tierney & Russell, 2009; Tierney et al., 2012) and rivers (e.g., Zhu

87   et al., 2011; De Jonge et al., 2015; French et al., 2015; Zell et al., 2015). Peterse et al.

88   (2009) compared the brGDGTs' distribution in Svalbard soils and nearby fjord

89   sediments, and found that concentrations of brGDGTs (0.01–0.20 μg/g dw) in fjord

90   sediments increased towards the open ocean and the distribution was strikingly different

91   from that in soil. Zhu et al. (2011) examined distributions of GDGTs in surface

92   sediments across a Yangtze River-dominated continental margin, and found evidence

93   for production of brGDGTs in the oxic East China Sea shelf water column and the

94   anoxic sediments/waters of the Lower Yangtze River. At the global scale, Fietz et al.

95   (2012) reported a significant correlation between concentrations of brGDGTs and

96   crenarchaeol ($p < 0.01$; $R^2 = 0.57–0.99$), suggesting that a common or mixed source for

97   brGDGTs and iGDGTs are actually commonplace in lacustrine and marine settings.

98   More recently, Sinninghe Damsté (2016) reported tetraethers in surface sediments from

99   43 stations in the Berau River delta (Kalimantan, Indonesia), and this result, combined

100 with data from other shelf systems, is coherent with the hypothesis that brGDGTs are

101 in situ produced   in shelf sediments especially at water depth of 50–300 m.

102   Fluvial inputs and wind are the most important pathways for transporting

103 terrestrial material into sea. On the continental shelf, fluvial discharge is more important

104 than atmospheric input because brGDGTs are either below the detection level

105 (Hopmans et al., 2004) or present at low abundance (Fietz et al., 2013; Weijers et al.,

106 2014). In the remote ocean where no direct impact from land erosion via rivers takes

107 place, eolian transport and in situ production are major contributors for brGDGTs.

108 Weijers et al. (2014) found that distributions of African dust-derived brGDGTs were

109 similar to those of soils but different from those of distal marine sediments, providing

110 a possibility to distinguish terrestrial vs. marine brGDGTs based on molecular

111 compositions. However, so far no robust molecular indicator is available for estimating

112 source of brGDGTs in marine environments. Considering this, we conduct a detailed

113 study on GDGTs in three cores from the Bohai Sea which are subject to the Yellow

114 River influence to different degree. Our purpose is to evaluate the source discerning

115 capability of different brGDGT parameters, from which the most sensitive parameter is

selected and applied for globally distributed marine sediments and soils to test whether it is valid at the global scale. Our study supplies an important step for improving accuracy of brGDGT-derived proxies and better understanding the marine carbon cycle and paleoenvironments.

2 Material and methods

2.1 Study area and sampling

The Bohai Sea is a semi-enclosed shallow sea in northern China, extending about 550 km from north to south and about 350 km from east to west. Its area is 77,000 km^2 and the mean depth is 18 m (Hu et al., 2009). The Bohai Strait at the eastern portion is the only passage connecting the Bohai Sea to the outer Yellow Sea. Several rivers, including Yellow River, the second largest river in the world in terms of sediment load (Milliman & Meade, 1983), drain into the Bohai Sea with a total annual runoff of 890×10^8 m^3. A 64 cm long gravity core (M1; 37.52°N, 119.32°E) was collected in July 2011, while other two cores, M3 (38.66°N, 119.54°E; 53 cm long) and M7 (39.53°N, 120.46°E; 60 cm long), were collected in July 2013 (Fig. 2). The sites M1, M3 and M7 are located in the south, the center and the north of the Bohai Sea, respectively. The cores were transported to the lab where they were sectioned at 1 or 2 cm interval. The age model was established on basis of ^{210}Pb and ^{137}Cs activity, showing that the bottom sediments are less than 100 years old (Wu et al., 2013 and unpublished data).

2.2 Lipid extraction and analyses

The detailed procedures for lipid extraction and GDGT analyses have been described in previous studies (Ding et al., 2015; Xiao et al., 2015). Briefly, the homogenous freeze-dried samples were ultrasonically extracted with dichloromethane (DCM)/methanol (3:1 v:v). The extracts were separated into nonpolar and polar fraction over silica gel columns. The latter fraction containing GDGTs was analyzed using an Agilent 1200 HPLC-atmospheric pressure chemical ionization-triple quadruple mass spectrometry (HPLC-APCI-MS) system. The separation of 5- and 6-methyl brGDGTs was achieved with two silica columns in sequence (150 mm×2.1 mm; 1.9 μm, Thermo

Finnigan; USA). The quantification was achieved by comparison of the respective protonated ion peak areas of each GDGT to the internal standard (C_{46} GDGT) in selected ion monitoring (SIM) mode. The protonated ions were m/z 1050, 1048, 1046, 1036, 1034, 1032, 1022, 1020, 1018 for brGDGTs, 1302, 1300, 1298, 1296, 1292 for iGDGTs and 744 for C_{46} GDGT.

2.3 Parameter calculation and statistics

The BIT, MBT, Methyl Index (MI), Degree of Cyclization (DC) of brGDGTs and weighted average number of cyclopentane moieties for tetramethylated brGDGTs (#Rings$_{tetra}$) were calculated according to the definitions of Hopmans et al. (2004), Weijers et al. (2007b), Zhang et al. (2011), Sinninghe Damsté et al. (2009) and Sinninghe Damsté (2016), respectively.

$$\text{BIT} = \frac{\text{Ia} + \text{IIa} + \text{IIIa}}{\text{Ia} + \text{IIa} + \text{IIIa} + \text{IV}} \quad (1)$$

$$\text{MBT} = \frac{\text{Ia} + \text{Ib} + \text{Ic}}{\text{Ia} + \text{IIa} + \text{IIIa} + \text{Ib} + \text{IIb} + \text{IIIb} + \text{Ic} + \text{IIc} + \text{IIIc}} \quad (2)$$

$$\text{MI} = 4 \times (\text{Ia} + \text{Ib} + \text{Ic}) + 5 \times (\text{IIa} + \text{IIb} + \text{IIb}) + 6 \times (\text{IIIa} + \text{IIIb} + \text{IIIc}) \quad (3)$$

$$\text{DC} = \frac{\text{Ib} + \text{IIb}}{\text{Ia} + \text{IIa} + \text{Ib} + \text{IIb}} \quad (4)$$

$$\text{\#Rings}_{tetra} = \frac{\text{Ib} + 2 \times \text{Ic}}{\text{Ia} + \text{Ib} + \text{Ic}} \quad (5)$$

where roman numbers denote relative abundance of compounds depicted in Fig. 1. In this study, we used two silica LC columns in tandem and successfully separated 5- and 6-methyl brGDGTs. However, many previous studies (e.g., Weijers et al., 2006) used one LC column and did not separate 5- and 6-methyl brGDGTs. Considering this, we combined 5-methyl and 6-methyl brGDGT as one compound in this study, for example, IIIa denotes the total abundance of brGDGT IIIa and IIIa' in figure 1.

An analysis of variance (ANOVA) was conducted for different types of samples to determine if they differ significantly from each other. The SPSS 16.0 software package (IBM, USA) was used for the statistical analysis. Squared Pearson correlation coefficients (R^2) were reported and a significance level is $p < 0.05$.

174   2.4 Data compilation of global soils and marine sediments

175   The dataset in this study is composed of relative abundance of GDGTs and derived

176   parameters from 1354 globally distributed soils and 589 marine sediments (Fig. 2 and

177   supplementary data). These sampling sites span a wide area from 75.00ºS to 79.28ºN

178   and 168.08ºW to 174.40ºE and the water depth ranges from 1.0 to 5521 m. The marine

179   samples are from the South China Sea (Hu et al., 2012; Jia et al., 2012; O'Brien et al.,

180   2014; Dong et al., 2015), Caribbean Sea (O'Brien et al., 2014), western equatorial

181   Pacific Ocean (O'Brien et al., 2014), southeast Pacific Ocean (Kaiser et al., 2015), the

182   Chukchi and Alaskan Beaufort Seas (Belicka & Harvey, 2009), eastern Indian Ocean

183   (Chen et al., 2014), East Siberian Arctic Shelf (Sparkes et al., 2015), Kara Sea (De

184   Jonge et al., 2015; De Jonge et al., 2016), Svalbard fjord (Peterse et al., 2009a), Red

185   Sea (Trommer et al., 2009), the southern Adriatic Sea (Leider et al., 2010), Columbia

186   estuary (French et al., 2015), globally distributed distal marine sediments (Weijers et

187   al., 2014) and the Bohai Sea (this study). Soil samples are from Svalbard (Peterse et al.,

188   2009b), Columbia (French et al., 2015), China (Yang et al., 2013; Yang et al., 2014a;

189   Yang et al., 2014b; Ding et al., 2015; Xiao et al., 2015; Hu et al., 2016), California

190   geothermal (Peterse et al., 2009b), France and Brazil (Huguet et al., 2010), western

191   Uganda (Loomis et al., 2011), the USA (Tierney et al., 2012), Tanzania (Coffinet et al.,

192   2014), Indonesia, Vietnam, Philippine, China and Italy (Mueller-Niggemann et al.,

193   2016) as well as globally distributed soils (Weijers et al., 2006; Peterse et al., 2012; De

194   Jonge et al., 2014).

195

196   3 Results and discussion

197   3.1 Distribution and source of brGDGTs in Bohai Sea

198   A series of iGDGTs including crenarchaeol and brGDGTs including 5-methyl and

199   6-methyl isomers were detected in Bohai Sea sediments. For brGDGTs, a total of 15

200   compounds were identified including three tetramethylated brGDGTs (Ia, Ib and Ic),

201   six pentamethylated brGDGTs (IIa, IIb, IIc, IIa', IIb' and IIc') and six hexamethylated

202   brGDGTs (IIIa, IIIb, IIIc, IIIa', IIIb' and IIIc'). In order to evaluate provenances of

203   brGDGTs, we calculated various parameters including the BIT index, percentages of

tetra-, penta- and hexa-methylated brGDGTs, #rings for tetramethylated brGDGTs, DC, MI, MBT, brGDGTs IIIa/IIa and Ia/IIa (Table 1). The values of the BIT index ranged from 0.27 to 0.76 in the core M1, which are much higher than that in the core M3 (0.04–0.25) and the core M7 (0.04–0.18). Such a difference is not surprising because the site M1 is closest to the Yellow River outflow, and receives more terrestrial organic carbon than the other (Fig. 2). However, the BIT index itself has no ability to determine the source of brGDGTs (terrestrial vs. aquatic) because brGDGTs and crenarchaeol used in this index are thought to be specific for soil organic carbon and marine organic carbon, respectively (Hopmans et al., 2004), although crenarchaeol is also present in soils at low abundance (Weijers et al., 2006). For individual brGDGTs, the core M1 is characterized by significantly higher percentage of brGDGT IIa (28±1%) than the core M2 (18±1%) and the core M3 (18±0%; Fig. 3). We performed ANOVA for a variety of brGDGTs' parameters. All results except from MI show a significant difference between Chinese soils and Bohai Sea sediments. The IIIa/IIa ratio is the most sensitive parameter which can completely separate the samples into four groups: Chinese soils (0.39±0.25; Mean±SD; same hereafter), M1 sediments (0.63±0.06), M3 sediments (1.16±0.12) and M7 sediments (0.93±0.07).

Three factors may account for the occurrence of higher IIIa/IIa ratio in the Bohai Sea sediments than Chinese soils: selective degradation during land to sea transport, admixture of river produced brGDGTs and in situ production of brGDGTs in sea. Huguet et al. (2008; 2009) reported that iGDGTs (i.e., crenarchaeol) were degraded at a rate of 2-fold higher than soil derived brGDGTs under long term oxygen exposure in the Madeira Abyssal Plain, leading to increase of the BIT index. Such selective degradation, however, cannot explain significant different IIIa/IIa ratio between the Chinese soils and Bohai Sea sediments because unlike crenarchaeol, both IIIa and IIa belong to brGDGTs with similar chemical structures and thus have similar degradation rates. In situ production of brGDGTs in rivers is a widespread phenomenon, and can change brGDGTs' composition in sea when they are transported there (e.g., Zhu et al., 2011; De Jonge et al., 2015; Zell et al., 2015). However, the study along lower Yellow River-estuary-coast transect suggests that brGDGTs in surface sediments are primarily

8

234　of land origin (Wu et al., 2014). In our study, the site M1 is adjacent to the Yellow River

235　mouth and receives the largest amount of terrestrial organic matter, causing lower

236　IIIa/IIa values (0.63±0.06). In contrast, the site M3 located in central Bohai Sea

237　comprises the least amount of terrestrial organic matter, resulting in higher IIIa/IIa

238　values (1.16±0.12). The intermediate IIIa/IIa values at the site M7 (0.93±0.07) is

239　attributed to moderate land erosion nearby northern Bohai Sea (Fig. 2). These GDGTs'

240　results, consistent with other terrestrial biomarkers such as C_{29} and C_{31} n-alkanes and

241　C_{29} sterol (data not showed here), suggest that the higher IIIa/IIa values in the Bohai

242　Sea sediments compared to Chinese soils (0.39±0.25) is most likely caused by in situ

243　production of brGDGTs.

244

245

246　3.2 Regional and global validation of brGDGT IIIa/IIa

247　　To test whether the IIIa/IIa ratio is valid in other environments, we apply it to the

248　dataset for Svalbard (Peterse et al., 2009a), the Yenisei River outflow (De Jonge et al.,

249　2015) and the East Siberian Arctic Shelf (Sparkes et al., 2015). Similar to Bohai Sea in

250　this study, the compounds brGDGT IIa and IIIa are also ubiquitously present in these

251　environments. By comparing the compositions of brGDGTs in Svalbard soils and

252　nearby fjord sediments, Peterse et al. (2009a) indicated that sedimentary organic matter

253　in fjords was predominantly from marine origin. A plot of BIT vs. IIIa/IIa (Fig. 4a)

254　clearly grouped the samples into two groups which correspond to soils (>0.75 for BIT

255　and <1.0 for IIIa/IIa) and marine sediments (<0.3 for BIT and >1.0 for IIIa/IIa). Another

256　line of evidence is from De Jonge et al. (2015) who examined brGDGTs in core lipids

257　(CLs) and intact polar lipids (IPLs) in the Yenisei River outflow. As the IPLs are rapidly

258　degraded in the environment, they can be used to trace living or recently living material,

259　while the CLs are generated via degradation of the IPLs after cell death (White et al.,

260　1979; Lipp et al., 2008). The compilation of brGDGTs' abundance from De Jonge et al.

261　(2015) shows significant difference of the IIIa/IIa ratio between the IPL fractions (>1.0)

262　and CL fractions (<0.8; Fig. 4b). Such disparity supports that brGDGTs produced in

263　marine environments have higher IIIa/IIa values because labile intact polar brGDGTs

are mainly produced in situ, whereas recalcitrant core brGDGTs are composed of more allochthonous terrestrial components. Sparkes et al. (2015) examined brGDGTs in surface sediments across the East Siberian Arctic Shelf (ESAS) including the Dmitry-Laptev Strait, Buor-Khaya Bay, ESAS nearshore and ESAS offshore. The plot of BIT vs. IIIa/IIa again results into two groups, one group with lower BIT values (<0.3) and higher IIIa/IIa values (0.8–2.3) mainly from ESAS offshore, and another group with higher BIT values (0.3–1.0) and lower IIIa/IIa values (0.4–0.9) from the Dmitry-Laptev Strait, Buor-Khaya Bay and ESAS nearshore (Fig. 4c). A strong linear correlation was observed between the IIIa/IIa ratio and the distance from river mouth (R^2=0.58; p<0.05; Fig. 4d), in accord with the data of the BIT index and $\delta^{13}C_{org}$ (Sparkes et al., 2015). All lines of evidence support that marine-derived brGDGTs have higher IIIa/IIa values than terrestrial derived brGDGTs.

We further extend the dataset for global scale (Fig. 5), showing that the IIIa/IIa ratio is still significantly higher in marine sediments than soils (p < 0.01). An exception was observed for Red Sea sediments which have unusually low IIIa/IIa values (0.39±0.21) compared to other marine sediments (>0.87). The Red Sea has a restricted connection to the Indian Ocean via the Bab el Mandeb Strait. This, combined with high insolation, low precipitation and strong winds result in surface water salinity up to 41 PSU in the south and 36 PSU in the north of the Red Sea (Sofianos et al., 2002). Under such extreme environment, distinct microbial populations may develop and produce GDGTs different from that in other marine settings (See Trommer et al., 2009 for details).

Overall, the global distribution of IIIa/IIa shows the highest values in many deep sea sediments (2.6–5.1), the lowest values in soils (<1.0), and intermediate values in sediments from bays, coastal areas or marginal seas (0.87–2.62; Fig. 5). These results are consistent with our data from the Bohai Sea, and confirm that the IIIa/IIa ratio is a useful proxy for tracing the source of brGDGTs in marine sediments at regional and global scales.

Why do marine sediments generally have higher IIIa/IIa values than soils? It has been reported that the relative of methyl groups positively correlates with soil pH and

negatively correlates with MAT (Weijers et al., 2007b; Peterse et al., 2012). The IIIa/IIa ratio is actually an abundance ratio of hexamethylated to pentamethylated brGDGT, and thus is also affected by ambient temperature and pH. Unlike iGDGTs which are well known to be mainly produced by Thaumarchaeota (Sinninghe Damsté et al., 2002; Schouten et al., 2008), the marine source of brGDGTs remains elusive. Here, we assume that marine organisms producing brGDGTs respond to ambient temperature in the same way as the brGDGTs producing soil bacteria, i.e., a negative correlation between relative number of methyl group of brGDGTs and ambient temperature. Because a large temperature gradient exists from surface to bottom water in the ocean, we need consider the location where brGDGTs are produced. If brGDGTs in marine environments are predominantly produced in euphotic zone, we would not observe a significant difference for the IIIa/IIa ratio between land and sea because both soils and marine sediments are globally distributed, leading to no systematic difference between soil temperature and sea surface temperature. Alternatively, if brGDGTs in marine sediments are partially derived from deep-water dwelling or benthic organisms, cold deep water (generally 1–2 $^{\circ}$C) would cause higher IIIa/IIa values in marine sediments, as we observed in this study. However, to the best of our knowledge, there is no study reporting in situ production of brGDGTs throughout the water column in ocean. Recent studies (Taylor et al., 2013; Kim et al., 2015) have suggested that Thaumarchaeota thriving in the deeper, bathypelagic water-column (>1000 m water depth) biosynthesized iGDGTs with different compositions as surface dwelling Thaumarchaeota, and thereby alter signals of TEX$_{86}$ in sediments. Besides temperature, pH can also alter compositions of brGDGTs (Weijers et al., 2007). Based on global soil data, the IIIa/IIa ratio shows a strong positive correlation with soil pH (R^2=0.51; Fig. 6). In our study, the majority of soils are acidic or neutral (pH<7.3) and only 8% of soil samples mainly from semi-arid and arid regions have pH of >8.0 (e.g., Yang et al., 2014a). In contrast, seawater is constantly alkaline with a mean pH of 8.2. With this systematic difference, bacteria living in soils tend to produce higher proportions of brGDGT IIa, whereas unknown marine organisms tend to biosynthesize higher proportions of brGDGT IIIa if they response to ambient pH in a similar way as soil bacteria in term of

324 biosynthesis of brGDGTs. It should be pointed out that unlike fairly stable pH of

325 overlying sea water, the pH of pore waters in marine sediments can vary significantly, which

326 may influence compositions of brGDGTs. Nevertheless, at current stage, the occurrence of

327 higher IIIa/IIa values in marine sediments is most likely attributed to the relative higher

328 pH and lower water temperature. Further studies are needed to disentangle relative

329 importance of these two factors.

330

331 3.3 Implication of IIIa/IIa on other brGDGT proxies

332 Because brGDGTs can be produced in marine settings, they are no longer specific

333 for soil organic matter, which inevitably affects brGDGT proxies (e.g., BIT, MBT/CBT).

334 The plot of BIT vs. IIIa/IIa on basis of global dataset shows that the IIIa/IIa ratio has

335 the value of <0.59 for 90% of soil samples and >0.92 for 90% of marine sediments (Fig.

336 7). Considering this fact, we propose that the IIIa/IIa ratio of <0.59 and >0.92 represents

337 terrestrial (or soil) and marine end-members, respectively. The BIT index has the value

338 of >0.67 for 90% of soils and <0.16 for 90% of marine sediments (Fig. 7). Overall, the

339 BIT index decreased with increasing IIIa/IIa values ($BIT = 1.08 \times 0.28^{\frac{IIIa}{IIa}} -$

340 $0.03; R^2 = 0.77;$ Fig. 7), suggesting that both the IIIa/IIa and BIT are useful indexes

341 for assessing soil organic carbon in marine settings. However, when the BIT index has

342 an intermediate value (i.e., 0.16 to 0.67), it is not valid to determine the provenance of

343 brGDGTs. For example, several marine samples having BIT values of ~0.35 show a

344 large range of IIIa/IIa (0.4 to 2.4; Fig. 7), suggesting that the source of brGDGTs can

345 vary case by case. Under this situation, the measurement of the IIIa/IIa ratio is strongly

346 recommended.

347 The different IIIa/IIa values between land and marine end-members may provide

348 an approach to quantify the contribution of soil organic carbon in marine sediments.

349 Similar to the BIT index, we used a binary mixing model to calculate percentage of soil

350 organic carbon (%OC$_{soil}$) as follow:

351 $$\%OC_{soil} = \left[\frac{[IIIa/IIa]_{sample} - [IIIa/IIa]_{marine}}{[IIIa/IIa]_{soil} - [IIIa/IIa]_{marine}} \right] * 100 \quad (6)$$

352 Where $[IIIa/IIa]_{sample}$, $[IIIa/IIa]_{soil}$ and $[IIIa/IIa]_{marine}$ are the abundance ratio of brGDGT

353 IIIa/IIa for samples, soils and marine sediments devoid of terrestrial influences,

354 respectively.

355 We applied this binary mixing model to the East Siberian Arctic Shelf because the

356 data of BIT, $\delta^{13}C_{org}$ and distance from river mouth are all available (Sparkes et al., 2015).

357 With the distance from river mouth increasing from 25 to >700 km, the BIT, IIIa/IIa

358 and $\delta^{13}C_{org}$ change from 0.95 to 0, 0.53 to 2.21 and –27.4‰ to –21.2‰, respectively,

359 reflecting spatial variability of sedimentary organic carbon sources. For the BIT index,

360 we used 0.97 and 0.01 as terrestrial and marine end-member values based on previous

361 studies for Arctic surrounding regions (De Jonge et al., 2014; Peterse et al., 2014),

362 which are similar to global average values (Hopmans et al., 2004). For $\delta^{13}C_{org}$, we chose

363 –27‰ and –20‰ as C3 terrestrial and marine organic carbon end-members (Meyers,

364 1997). For the IIIa/IIa ratio, we used a global average value of marine sediments (1.6)

365 and soils (0.24), respectively, based on this study. By applying these end-member

366 values into Eq. 6, we calculated percentage of soil organic carbon (%OC$_{soil}$). We

367 removed a few data points if their calculated %OC$_{soil}$ were greater than 100% or below

368 0%. It should be noted that the end-member value will affect quantitative results, but

369 does not change a general trend of %OC$_{soil}$. The results based on all three parameters

370 show a decreasing trend seawards (Fig. 8). However, the %OC$_{soil}$ based on $\delta^{13}C_{org}$ is

371 the highest (75±18%), followed by that from the IIIa/IIa ratio (58±15%) and then that

372 from the BIT index (43±27%). This difference have been explained by that $\delta^{13}C_{org}$ is a

373 bulk proxy for marine vs. terrestrial influence of sedimentary organic carbon (SOC),

374 whereas the BIT index is for a portion of the bulk SOC, i.e., soil OC (Walsh et al., 2008)

375 or fluvial OC (Sparkes et al., 2015). For the estimated %OC$_{soil}$, $\delta^{13}C_{org}$ presents a

376 stronger positive correlation with the IIIa/IIa ratio (R^2=0.49) than the BIT index

377 (R^2=0.45), suggesting that the IIIa/IIa ratio may serve a better proxy for quantifying

378 soil organic carbon than the BIT index because it is less affected by selective

379 degradation of branched vs. isoprenoid GDGTs and high production of crenarchaea in

380 marine environments (Smith et al., 2012).

381

4 Conclusions

Our investigation in brGDGTs in three Bohai Sea cores and globally distributed soils and marine sediments shows that the brGDGTs IIIa/IIa ratio is lower than 0.59 in 90% of soils, but higher than 0.92 in 90% of marine sediments devoid of significant terrestrial inputs, supporting that the IIIa/IIa is a sensitive proxy for assessing soil vs. marine derived brGDGTs at regional and global scales. The in situ production of brGDGTs in marine environments is a ubiquitous phenomenon, which is particularly important for those marine sediments with low BIT index (<0.16) where brGDGTs are primarily of marine origin. A systemic difference of the IIIa/IIa value between soils and marine sediments reflects an effect of pH or the combined effect of pH and temperature on the biosynthesis of brGDGTs by source organisms. Given these facts, we recommend to calculate the IIIa/IIa ratio before estimating organic carbon source, paleo-soil pH and MAT based on the BIT and MBT/CBT proxies. We also note a relatively large scatter of the IIIa/IIa ratio within both terrestrial and marine realms, and recently reported different environmental responses of 5-methyl vs. 6-methyl brGDGTs (e.g., De Jonge et al., 2014, 2016; Xiao et al., 2015). As a result, the separation of these two types of isomers is needed in future studies in order to develop more accurate brGDGTs-based proxies.

References

Belicka, L.L., Harvey, H.R., The sequestration of terrestrial organic carbon in Arctic Ocean sediments: A comparison of methods and implications for regional carbon budgets. Geochim. Cosmochim. Acta, 73, 6231–6248, 2009.

Blaga, C.I., Reichart, G.J., Vissers, E.W., Lotter, A.F., Anselmetti, F.S., Damste, J.S.S., Seasonal changes

412   in glycerol dialkyl glycerol tetraether concentrations and fluxes in a perialpine lake:

413   Implications for the use of the TEX_{86} and BIT proxies. Geochim. Cosmochim. Acta, 75, 6416–

414   6428, 2011.

415 Chen, W., Mohtadi, M., Schefuß, E., Mollenhauer, G., Organic-geochemical proxies of sea surface

416   temperature in surface sediments of the tropical eastern Indian Ocean. Deep Sea Research Part

417   I: Oceanographic Research Papers, 88, 17–29, 2014.

418 Coffinet, S., Huguet, A., Williamson, D., Fosse, C., Derenne, S., Potential of GDGTs as a temperature

419   proxy along an altitudinal transect at Mount Rungwe (Tanzania). Org. Geochem., 68, 82–89,

420   2014.

421 De Jonge, C., Hopmans, E.C., Stadnitskaia, A., Rijpstra, W.I.C., Hofland, R., Tegelaar, E., Sinninghe

422   Damsté, J.S., Identification of novel penta- and hexamethylated branched glycerol dialkyl

423   glycerol tetraethers in peat using HPLC–MS2, GC–MS and GC–SMB-MS. Org. Geochem., 54,

424   78–82, 2013.

425 De Jonge, C., Hopmans, E.C., Zell, C.I., Kim, J.-H., Schouten, S., Sinninghe Damsté, J.S., Occurrence

426   and abundance of 6-methyl branched glycerol dialkyl glycerol tetraethers in soils: Implications

427   for palaeoclimate reconstruction. Geochim. Cosmochim. Acta, 141, 97–112, 2014.

428 De Jonge, C., Stadnitskaia, A., Cherkashov, G., Sinninghe Damsté, J.S., Branched glycerol dialkyl

429   glycerol tetraethers and crenarchaeol record post-glacial sea level rise and shift in source of

430   terrigenous brGDGTs in the Kara Sea (Arctic Ocean). Org. Geochem., 92, 42–54, 2016.

431 De Jonge, C., Stadnitskaia, A., Hopmans, E.C., Cherkashov, G., Fedotov, A., Streletskaya, I.D., Vasiliev,

432   A.A., Sinninghe Damsté, J.S., Drastic changes in the distribution of branched tetraether lipids

433   in suspended matter and sediments from the Yenisei River and Kara Sea (Siberia): Implications

434   for the use of brGDGT-based proxies in coastal marine sediments. Geochim. Cosmochim. Acta,

435   165, 200–225, 2015.

436 Ding, S., Xu, Y., Wang, Y., He, Y., Hou, J., Chen, L., He, J.S., Distribution of branched glycerol dialkyl

437   glycerol tetraethers in surface soils of the Qinghai–Tibetan Plateau: implications of brGDGTs-

438   based proxies in cold and dry regions. Biogeosciences, 12, 3141–3151, 2015.

439 Dong, L., Li, Q., Li, L., Zhang, C.L., Glacial–interglacial contrast in MBT/CBT proxies in the South

440   China Sea: Implications for marine production of branched GDGTs and continental

441   teleconnection. Org. Geochem., 79, 74–82, 2015.

442 Fietz, S., Huguet, C., Bendle, J., Escala, M., Gallacher, C., Herfort, L., Jamieson, R., Martínez-Garcia,
443   A., McClymont, E.L., Peck, V.L., Prahl, F.G., Rossi, S., Rueda, G., Sanson-Barrera, A., Rosell-
444   Melé, A., Co-variation of crenarchaeol and branched GDGTs in globally-distributed marine and
445   freshwater sedimentary archives. Glob. Planet. Change, 92, 275–285, 2012.

446 Fietz, S., Prahl, F.G., Moraleda, N., Rosell-Melé, A., Eolian transport of glycerol dialkyl glycerol
447   tetraethers (GDGTs) off northwest Africa. Org. Geochem., 64, 112–118, 2013.

448 French, D.W., Huguet, C., Turich, C., Wakeham, S.G., Carlson, L.T., Ingalls, A.E., Spatial distributions
449   of core and intact glycerol dialkyl glycerol tetraethers (GDGTs) in the Columbia River Basin
450   and Willapa Bay, Washington: Insights into origin and implications for the BIT index. Org.
451   Geochem., 88, 91–112, 2015.

452 Herfort, L., Schouten, S., Boon, J.P., Woltering, M., Baas, M., Weijers, J.W.H., Damsté, J.S.S.,
453   Characterization of transport and deposition of terrestrial organic matter in the southern North
454   Sea using the BIT index. Limnol. Oceanogr., 51, 2196–2205, 2006.

455 Hopmans, E.C., Weijers, J.W.H., Schefuss, E., Herfort, L., Damste, J.S.S., Schouten, S., A novel proxy
456   for terrestrial organic matter in sediments based on branched and isoprenoid tetraether lipids.
457   Earth Planet. Sci. Lett., 224, 107–116, 2004.

458 Hu, J., Meyers, P.A., Chen, G., Peng, P.A., Yang, Q., Archaeal and bacterial glycerol dialkyl glycerol
459   tetraethers in sediments from the Eastern Lau Spreading Center, South Pacific Ocean. Org.
460   Geochem., 43, 162–167, 2012.

461 Hu, J., Zhou, H., Peng, P.A., Spiro, B., Seasonal variability in concentrations and fluxes of glycerol
462   dialkyl glycerol tetraethers in Huguangyan Maar Lake, SE China: Implications for the
463   applicability of the MBT–CBT paleotemperature proxy in lacustrine settings. Chem. Geol., 420,
464   200–212, 2016.

465 Hu, L., Guo, Z., Feng, J., Yang, Z., Fang, M., Distributions and sources of bulk organic matter and
466   aliphatic hydrocarbons in surface sediments of the Bohai Sea, China. Mar. Chem., 113, 197–
467   211, 2009.

468 Huguet, A., Fosse, C., Metzger, P., Fritsch, E., Derenne, S., Occurrence and distribution of extractable
469   glycerol dialkyl glycerol tetraethers in podzols. Org. Geochem., 41, 291–301, 2010.

470 Huguet, C., de Lange, G.J., Gustafsson, Ö., Middelburg, J.J., Sinninghe Damsté, J.S., Schouten, S.,
471   Selective preservation of soil organic matter in oxidized marine sediments (Madeira Abyssal

472   Plain). Geochim. Cosmochim. Acta, 72, 6061–6068, 2008.

473   Huguet, C., Kim, J.-H., de Lange, G.J., Sinninghe Damsté, J.S., Schouten, S., Effects of long term oxic

474   degradation on the , TEX_{86} and BIT organic proxies. Org. Geochem., 40, 1188–1194, 2009.

475   Jia, G., Zhang, J., Chen, J., Peng, P.A., Zhang, C.L., Archaeal tetraether lipids record subsurface water

476   temperature in the South China Sea. Org. Geochem., 50, 68–77, 2012.

477   Kaiser, J., Schouten, S., Kilian, R., Arz, H.W., Lamy, F., Sinninghe Damsté, J.S., Isoprenoid and branched

478   GDGT-based proxies for surface sediments from marine, fjord and lake environments in Chile.

479   Org. Geochem., 89, 117–127, 2015.

480   Kim, J.-H., Schouten, S., Rodrigo-Gámiz, M., Rampen, S., Marino, G., Huguet, C., Helmke, P., Buscail,

481   R., Hopmans, E.C., Pross, J., Sangiorgi, F., Middelburg, J.B.M., Sinninghe Damsté, J.S.,

482   Influence of deep-water derived isoprenoid tetraether lipids on the paleothermometer in the

483   Mediterranean Sea. Geochim. Cosmochim. Acta, 150, 125–141, 2015.

484   Kim, J.H., Meer, J.V.D., Schouten, S., Helmke, P., Willmott, V., Sangiorgi, F., Koç, N., Hopmans, E.C.,

485   Damsté, J.S.S., New indices and calibrations derived from the distribution of crenarchaeal

486   isoprenoid tetraether lipids: Implications for past sea surface temperature reconstructions.

487   Geochim. Cosmochim. Acta, 74, 4639–4654, 2010.

488   Kim, J.H., Schouten, S., Buscail, R., Ludwig, W., Bonnin, J., Sinninghe Damsté, J.S., Bourrin, F., Origin

489   and distribution of terrestrial organic matter in the NW Mediterranean (Gulf of Lions):

490   Exploring the newly developed BIT index. Geochem. Geophy. Geosy., 7, 220–222, 2006.

491   Leider, A., Hinrichs, K.U., Mollenhauer, G., Versteegh, G.J.M., Core-top calibration of the lipid-based

492   UK'37 and TEX_{86} temperature proxies on the southern Italian shelf (SW Adriatic Sea, Gulf of

493   Taranto). Earth Planet. Sci. Lett., 300, 112–124, 2010.

494   Lincoln, S.A., Wai, B., Eppley, J.M., Church, M.J., Summons, R.E., Delong, E.F., Planktonic

495   Euryarchaeota are a significant source of archaeal tetraether lipids in the ocean. Proc. Natl. Acad.

496   Sci., 111, 9858–9863, 2014.

497   Lipp, J.S., Morono, Y., Inagaki, F., Hinrichs, K.U., Significant contribution of Archaea to extant biomass

498   in marine subsurface sediments. Nature, 454, 991–994, 2008.

499   Liu, X.-L., Zhu, C., Wakeham, S.G., Hinrichs, K.-U., In situ production of branched glycerol dialkyl

500   glycerol tetraethers in anoxic marine water columns. Mar. Chem., 166, 1–8, 2014.

501   Loomis, S.E., Russell, J.M., Damsté, J.S.S., Distributions of branched GDGTs in soils and lake sediments

from western Uganda: Implications for a lacustrine paleothermometer. Org. Geochem., 42, 739–751, 2011.

Meyers, P.A., Organic geochemical proxies of paleoceanographic, paleolimnologic, and paleoclimatic processes. Org. Geochem., 27, 213–250, 1997.

Milliman, J.D., Meade, R.H., World-wide delivery of river sediment to the oceans. J. Geol., 91, 1–21, 1983.

Mueller-Niggemann, C., Utami, S.R., Marxen, A., Mangelsdorf, K., Bauersachs, T., Schwark, L., Distribution of tetraether lipids in agricultural soils–differentiation between paddy and upland management. Biogeosciences, 13, 1647–1666, 2016.

O'Brien, C.L., Foster, G.L., Martínez-Botí, M.A., Abell, R., Rae, J.W.B., Pancost, R.D., High sea surface temperatures in tropical warm pools during the Pliocene. Nat Geosci, 7, 606–611, 2014.

Peterse, F., Kim, J.-H., Schouten, S., Kristensen, D.K., Koç, N., Sinninghe Damsté, J.S., Constraints on the application of the MBT/CBT palaeothermometer at high latitude environments (Svalbard, Norway). Org. Geochem., 40, 692–699, 2009a.

Peterse, F., Schouten, S., van der Meer, J., van der Meer, M.T.J., Sinninghe Damsté, J.S., Distribution of branched tetraether lipids in geothermally heated soils: Implications for the MBT/CBT temperature proxy. Org. Geochem., 40, 201–205, 2009b.

Peterse, F., van der Meer, J., Schouten, S., Weijers, J.W.H., Fierer, N., Jackson, R.B., Kim, J.-H., Sinninghe Damsté, J.S., Revised calibration of the MBT–CBT paleotemperature proxy based on branched tetraether membrane lipids in surface soils. Geochim. Cosmochim. Acta, 96, 215–229, 2012.

Peterse, F., Vonk, J.E., Holmes, R.M., Giosan, L., Zimov, N., Eglinton, T.I., Branched glycerol dialkyl glycerol tetraethers in Arctic lake sediments: Sources and implications for paleothermometry at high latitudes. J. Geophys. Res.-Biogeo., 119, 1738–1754, 2014.

Schouten, S., Hopmans, E.C., Baas, M., Boumann, H., Standfest, S., Konneke, M., Stahl, D.A., Sinninghe Damste, J.S., Intact membrane lipids of "Candidatus Nitrosopumilus maritimus," a cultivated representative of the cosmopolitan mesophilic group I Crenarchaeota. Appl. Environ. Microbiol., 74, 2433–2440, 2008.

Schouten, S., Hopmans, E.C., Schefuß, E., Sinninghe Damsté, J.S., Distributional variations in marine crenarchaeotal membrane lipids: a new tool for reconstructing ancient sea water temperatures?

532   Earth Planet. Sci. Lett., 204, 265–274, 2002.

533 Schouten, S., Hopmans, E.C., Sinninghe Damsté, J.S., The organic geochemistry of glycerol dialkyl

534   glycerol tetraether lipids: A review. Org. Geochem., 54, 19–61, 2013.

535 Sinninghe Damsté, J.S., Spatial heterogeneity of sources of branched tetraethers in shelf systems: The

536   geochemistry of tetraethers in the Berau River delta (Kalimantan, Indonesia). Geochim.

537   Cosmochim. Acta, 186, 13–31, 2016.

538 Sinninghe Damsté, J.S., Hopmans, E.C., Pancost, R.D., Schouten, S., Geenevasen, J.A.J., Newly

539   discovered non-isoprenoid glycerol dialkyl glycerol tetraether lipids in sediments. Chem.

540   Commun., 17, 1683–1684, 2000.

541 Sinninghe Damsté, J.S., Ossebaar, J., Abbas, B., Schouten, S., Verschuren, D., Fluxes and distribution of

542   tetraether lipids in an equatorial African lake: Constraints on the application of the TEX_{86}

543   palaeothermometer and BIT index in lacustrine settings. Geochim. Cosmochim. Acta, 73, 4232–

544   4249, 2009.

545 Sinninghe Damsté, J.S., Ossebaar, J., Schouten, S., Verschuren, D., Altitudinal shifts in the branched

546   tetraether lipid distribution in soil from Mt. Kilimanjaro (Tanzania): Implications for the

547   MBT/CBT continental palaeothermometer. Org. Geochem., 39, 1072–1076, 2008.

548 Sinninghe Damsté, J.S., Rijpstra, W.I.C., Hopmans, E.C., Weijers, J.W.H., Foesel, B.U., Overmann, J.,

549   Dedysh, S.N., 13,16-Dimethyl Octacosanedioic Acid (iso-Diabolic Acid), a Common

550   Membrane-Spanning Lipid of Acidobacteria Subdivisions 1 and 3. Appl. Environ. Microbiol.,

551   77, 4147–4154, 2011.

552 Sinninghe Damsté, J.S., Schouten, S., Hopmans, E.C., van Duin, A.C.T., Geenevasen, J.A.J.,

553   Crenarchaeol: the characteristic core glycerol dibiphytanyl glycerol tetraether membrane lipid

554   of cosmopolitan pelagic crenarchaeota. J. Lipid Res., 43, 1641–1651, 2002.

555 Smith, R.W., Bianchi, T.S., Li, X., A re-evaluation of the use of branched GDGTs as terrestrial

556   biomarkers: Implications for the BIT Index. Geochim. Cosmochim. Acta, 80, 14–29, 2012.

557 Sofianos, S.S., Johns, W.E., Murray, S.P., Heat and freshwater budgets in the Red Sea from direct

558   observations at Bab el Mandeb. Deep Sea Res. Part II: Top. Stud. Oceanogr., 49, 1323–1340,

559   2002.

560 Sparkes, R.B., Doğrul Selver, A., Bischoff, J., Talbot, H.M., Gustafsson, Ö., Semiletov, I.P., Dudarev,

561   O.V., van Dongen, B.E., GDGT distributions on the East Siberian Arctic Shelf: implications for

562   organic carbon export, burial and degradation. Biogeosciences, 12, 3753–3768, 2015.

563   Taylor, K.W.R., Huber, M., Hollis, C.J., Hernandez-Sanchez, M.T., Pancost, R.D., Re-evaluating modern

564   and Palaeogene GDGT distributions: Implications for SST reconstructions. Glob. Planet.

565   Change, 108, 158–174, 2013.

566   Tierney, J.E., Russell, J.M., Distributions of branched GDGTs in a tropical lake system: Implications for

567   lacustrine application of the MBT/CBT paleoproxy. Org. Geochem., 40, 1032–1036, 2009.

568   Tierney, J.E., Schouten, S., Pitcher, A., Hopmans, E.C., Sinninghe Damsté, J.S., Core and intact polar

569   glycerol dialkyl glycerol tetraethers (GDGTs) in Sand Pond, Warwick, Rhode Island (USA):

570   Insights into the origin of lacustrine GDGTs. Geochim. Cosmochim. Acta, 77, 561–581, 2012.

571   Trommer, G., Siccha, M., Meer, M.T.J.V.D., Schouten, S., Damsté, J.S.S., Schulz, H., Hemleben, C.,

572   Kucera, M., Distribution of Crenarchaeota tetraether membrane lipids in surface sediments from

573   the Red Sea. Org. Geochem., 40, 724–731, 2009.

574   Walsh, E.M., Ingalls, A.E., Keil, R.G., Sources and transport of terrestrial organic matter in Vancouver

575   Island fjords and the Vancouver-Washington Margin: A multiproxy approach using d13Corg,

576   lignin phenols, and the ether lipid BIT index. Limnol. Oceanogr., 53, 1054–1063, 2008.

577   Weijers, J.W.H., Schefuß, E., Kim, J.-H., Sinninghe Damsté, J.S., Schouten, S., Constraints on the

578   sources of branched tetraether membrane lipids in distal marine sediments. Org. Geochem., 72,

579   14–22, 2014.

580   Weijers, J.W.H., Schefuß, E., Schouten, S., Damsté, J.S.S., Coupled thermal and hydrological evolution

581   of tropical Africa over the last deglaciation. Science, 315, 1701–1704, 2007a.

582   Weijers, J.W.H., Schouten, S., Donker, J.C.V.D., Hopmans, E.C., Damsté, J.S.S., Environmental controls

583   on bacterial tetraether membrane lipid distribution in soils. Geochim. Cosmochim. Acta, 71,

584   703–713, 2007b.

585   Weijers, J.W.H., Schouten, S., Spaargaren, O.C., Sinninghe Damsté, J.S., Occurrence and distribution of

586   tetraether membrane lipids in soils: Implications for the use of the TEX_{86} proxy and the BIT

587   index. Org. Geochem., 37, 1680–1693, 2006.

588   White, D.C., Davis, W.M., Nickels, J.S., King, J.D., Bobbie, R.J., Determination of the sedimentary

589   microbial biomass by extractible lipid phosphate. Oecologia, 40, 51–62, 1979.

590   Wu, W., Ruan, J., Ding, S., Zhao, L., Xu, Y., Yang, H., Ding, W., Pei, Y., Source and distribution of

591   glycerol dialkyl glycerol tetraethers along lower Yellow River-estuary–coast transect. Mar.

592   Chem., 158, 17–26, 2014.

593   Wu, W., Zhao, L., Pei, Y., Ding, W., Yang, H., Xu, Y., Variability of tetraether lipids in Yellow River-
594   dominated continental margin during the past eight decades: Implications for organic matter
595   sources and river channel shifts. Org. Geochem., 60, 33–39, 2013.

596   Xiao, W., Xu, Y., Ding, S., Wang, Y., Zhang, X., Yang, H., Wang, G., Hou, J., Global calibration of a
597   novel, branched GDGT-based soil pH proxy. Org. Geochem., 89, 56–60, 2015.

598   Yang, G., Zhang, C.L., Xie, S., Chen, Z., Gao, M., Ge, Z., Yang, Z., Microbial glycerol dialkyl glycerol
599   tetraethers lipids from water and soil at the Three Gorges Dam on the Yangtze River. Org.
600   Geochem., 56, 40–50, 2013.

601   Yang, H., Pancost, R.D., Dang, X., Zhou, X., Evershed, R.P., Xiao, G., Tang, C., Gao, L., Guo, Z., Xie,
602   S., Correlations between microbial tetraether lipids and environmental variables in Chinese soils:
603   Optimizing the paleo-reconstructions in semi-arid and arid regions. Geochim. Cosmochim. Acta,
604   126, 49–69, 2014a.

605   Yang, H., Pancost, R.D., Tang, C., Ding, W., Dang, X., Xie, S., Distributions of isoprenoid and branched
606   glycerol dialkanol diethers in Chinese surface soils and a loess–paleosol sequence: Implications
607   for the degradation of tetraether lipids. Org. Geochem., 66, 70-79, 2014b.

608   Zell, C., Kim, J.-H., Dorhout, D., Baas, M., Sinninghe Damsté, J.S., Sources and distributions of
609   branched tetraether lipids and crenarchaeol along the Portuguese continental margin:
610   Implications for the BIT index. Cont. Shelf. Res., 96, 34–44, 2015.

611   Zell, C., Kim, J.-H., Hollander, D., Lorenzoni, L., Baker, P., Silva, C.G., Nittrouer, C., Sinninghe Damsté,
612   J.S., Sources and distributions of branched and isoprenoid tetraether lipids on the Amazon shelf
613   and fan: Implications for the use of GDGT-based proxies in marine sediments. Geochim.
614   Cosmochim. Acta, 139, 293–312, 2014.

615   Zhang, Y.G., Zhang, C.L., Liu, X.-L., Li, L., Hinrichs, K.-U., Noakes, J.E., Methane Index: A tetraether
616   archaeal lipid biomarker indicator for detecting the instability of marine gas hydrates. Earth
617   Planet. Sci. Lett., 307, 525-534, 2011.

618   Zhu, C., Wakeham, S.G., Elling, F.J., Basse, A., Mollenhauer, G., Versteegh, G.J.M., ouml, nneke, M.,
619   Hinrichs, K.U., Stratification of archaeal membrane lipids in the ocean and implications for
620   adaptation and chemotaxonomy of planktonic archaea. Environ. Microbiol., DOI:
621   10.1111/1462-2920.13289, 2016.

622   Zhu, C., Weijers, J.W.H., Wagner, T., Pan, J.M., Chen, J.F., Pancost, R.D., Sources and distributions of

623   tetraether lipids in surface sediments across a large river-dominated continental margin. Org.

624   Geochem., 42, 376–386, 2011.

625

626

627

628

629

630

631

632

633

634

635
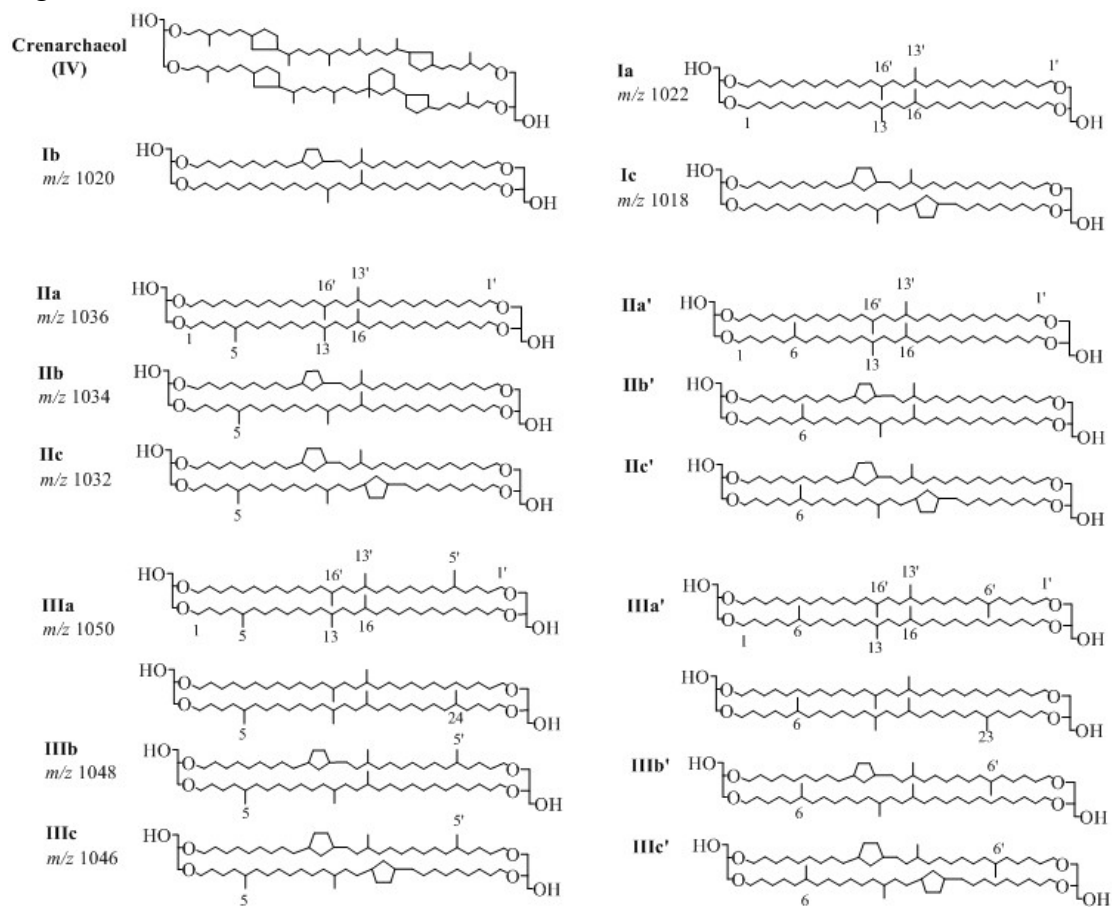
636

637

638

639

640

641

642

643

644

645

646

647

648

649

650

651

652   Fig. 1. Chemical structures of branched GDGTs and crenarchaeol.

653
654
655
656
657
658
659
660
661
662
663
664
665
666
667

668　　Fig. 2. Location of the samples used in this study. White circles and black circles

669　　indicate the soils and marine sediments, respectively. Red crosses denote three sediment

670　　cores (M1, M3 and M7) in the Bohai Sea. YR is the Yellow River.
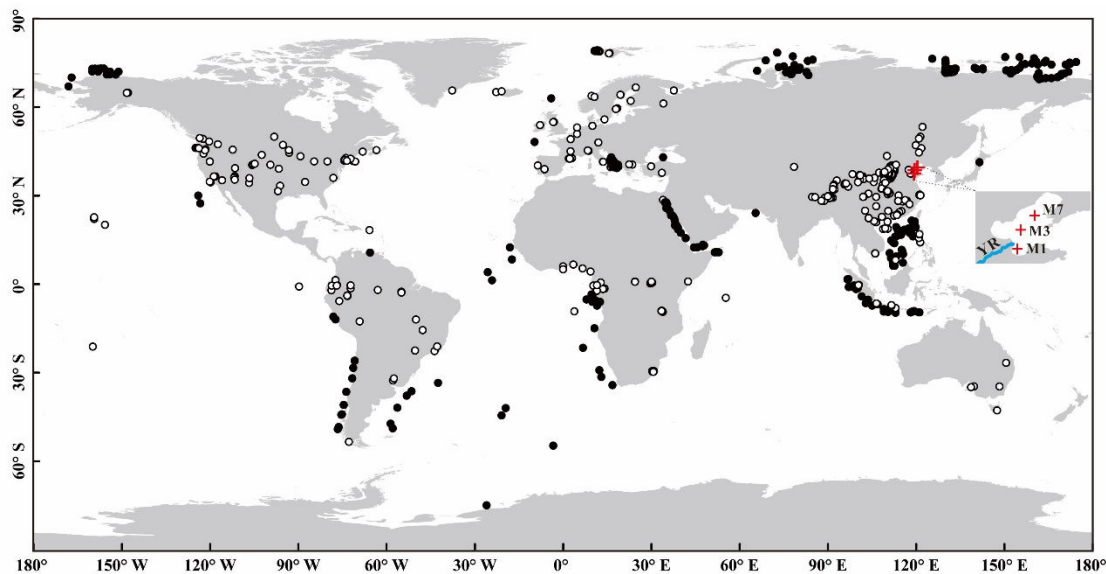
671

672

673

674

675

676

677

678

679

680

681

682

683

684

685

686

687

688

689 Fig. 3. Averaged percentages of individual brGDGTs in soils (a), core M1 (b), M3 (c)

690 and M7 (d). The soil data are from Yang et al. (2014a).
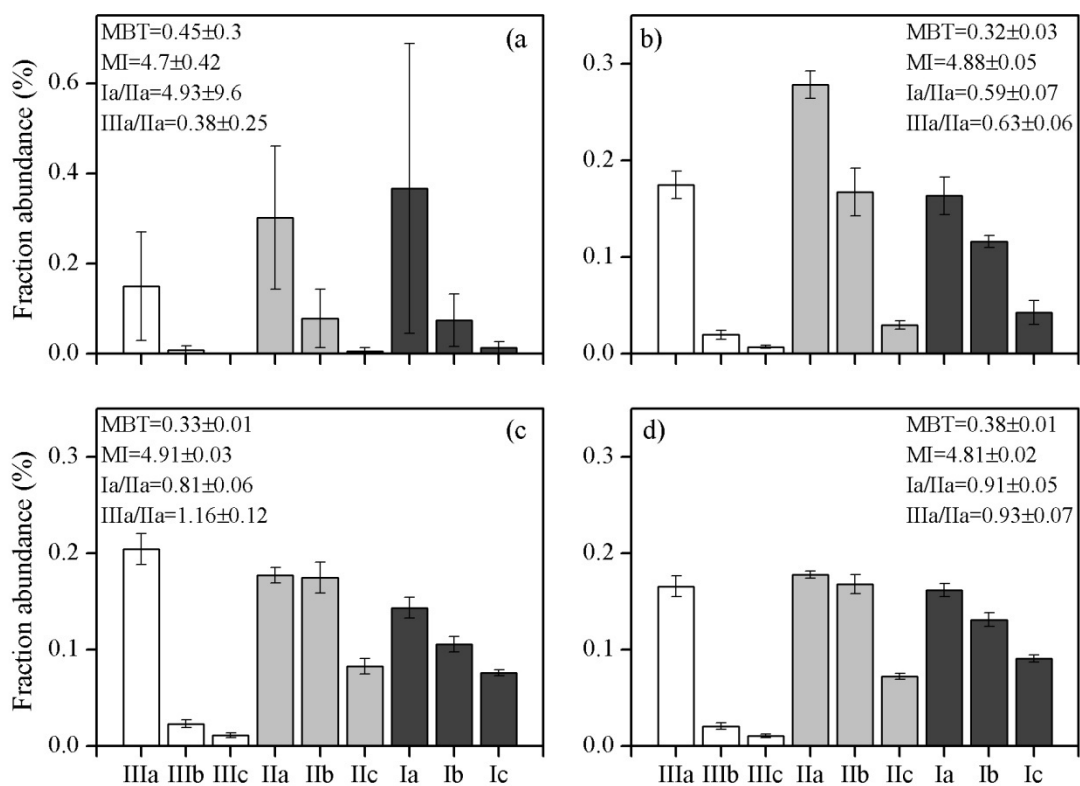
691

692

693

694

695

696

697

698

699

700

701

702

703

704

705

Fig. 4. a) The relationship between brGDGT IIIa/IIa ratio and the BIT index of samples from Peterse et al. (2009a); b) histograms of brGDGT IIIa/IIa ratio of the core lipids (CLs) and intact polar lipids (IPLs) in samples from De Jonge et al. (2015); c) the relationship between brGDGT IIIa/IIa ratio and the BIT index in samples from Sparkes et al. (2015); d) the relationship between brGDGT IIIa/IIa ratio and distance from river mouth in samples from Sparkes et al. (2015).
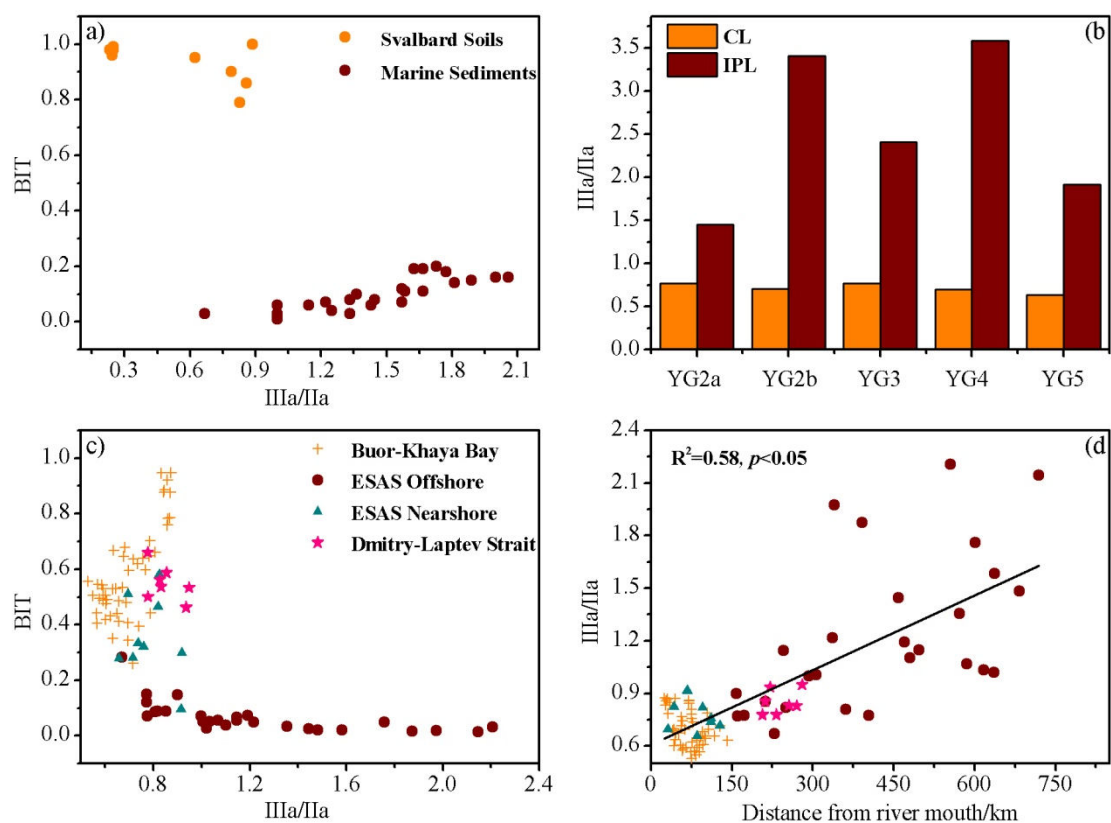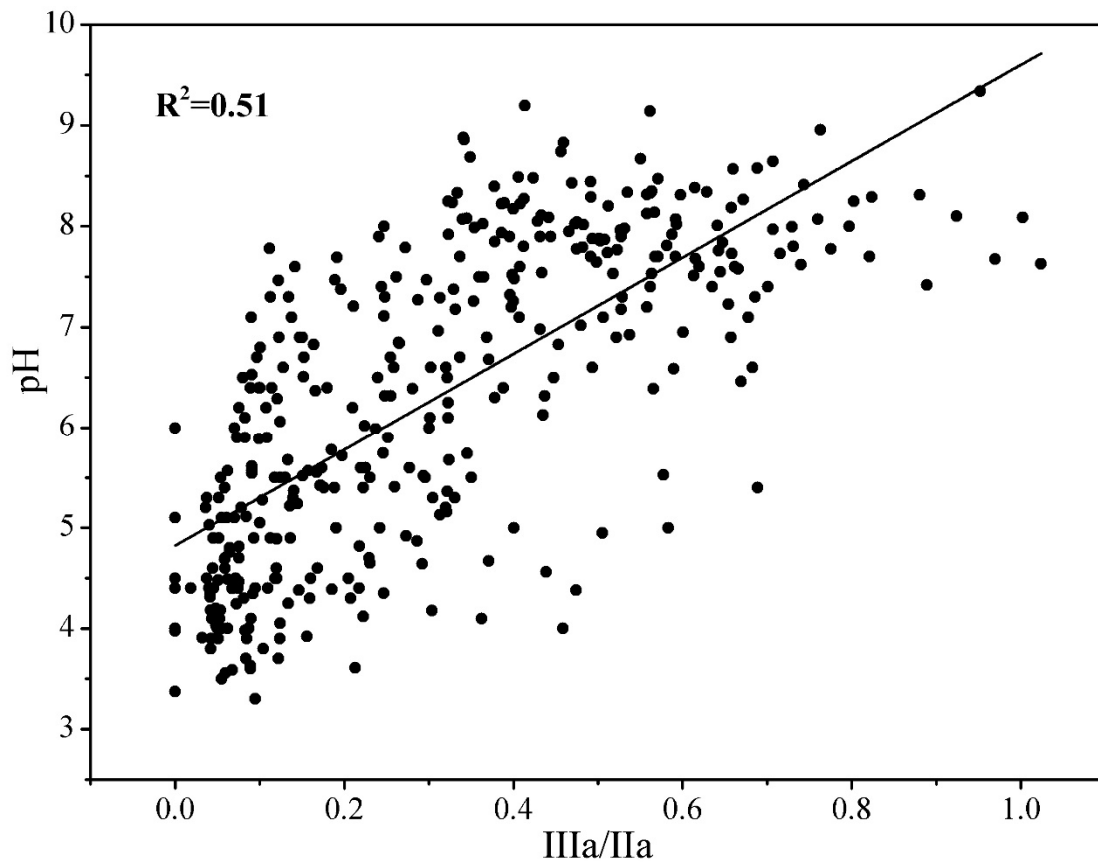
723 Fig. 5. Global distribution pattern of brGDGT IIIa/IIa ratio in soils and marine

724 sediments.

Legend: 0.00-0.39, 0.39-0.87, 0.87-1.32, 1.32-1.86, 1.86-2.62, 2.62-5.13
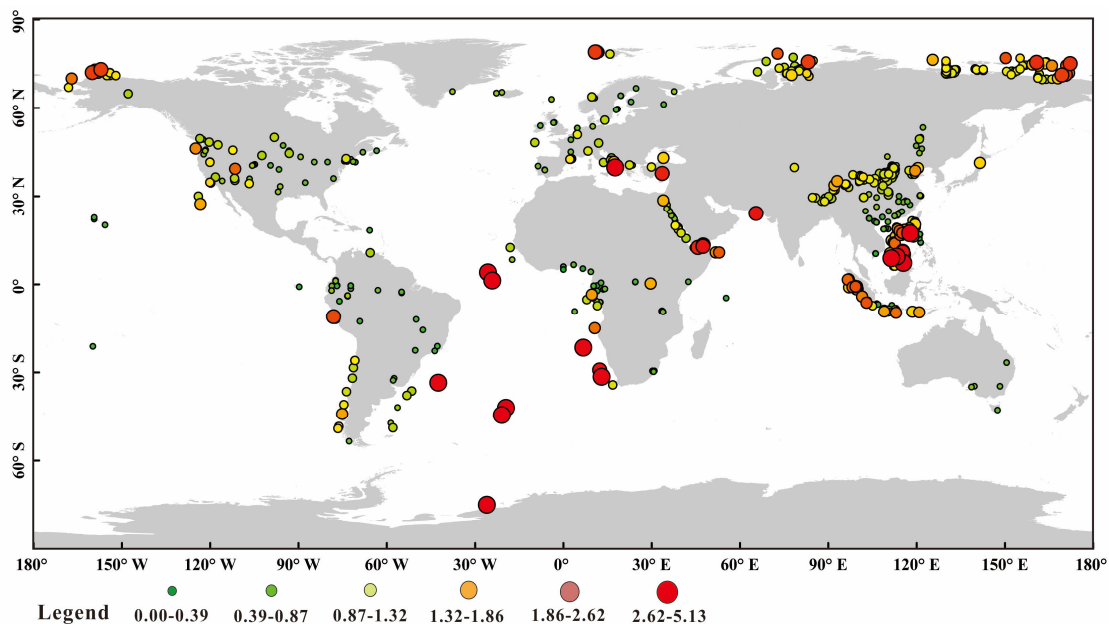
744 Fig. 6 a plot showing a positive correlation between soil pH and IIIa/IIa. The data are from

745 Peterse et al. (2012) and this study.

746
747
748
749
750
751
752
753
754
755
756
757
758
759
760

761   Fig. 7. Relationship between the IIIa/IIa ratio and the BIT index of globally distributed

762   samples: soils (orange circle) and marine sediments (red circle). Dashed lines represent

763   lower or upper threshold values for 90% of soils/sediments.
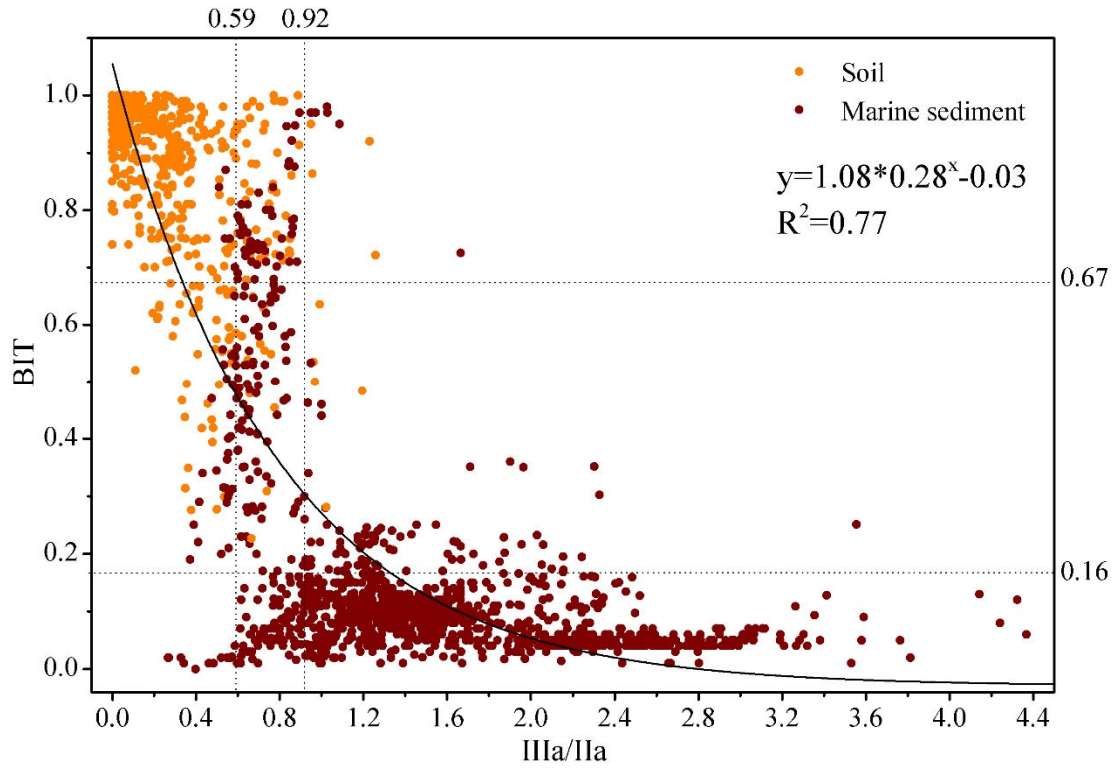
764

765

766

767

768

769

770

771

772

773

774

775

776

777

778

Fig. 8. Percentage of soil organic carbon (%OC$_{soil}$) or terrestrial organic carbon (%OC$_{terr}$) based on a binary mixing model of BIT (a), $\delta^{13}C_{org}$ (b) and IIIa/IIa (c) for the East Siberian Arctic Shelf (Sparkes et al., 2015).
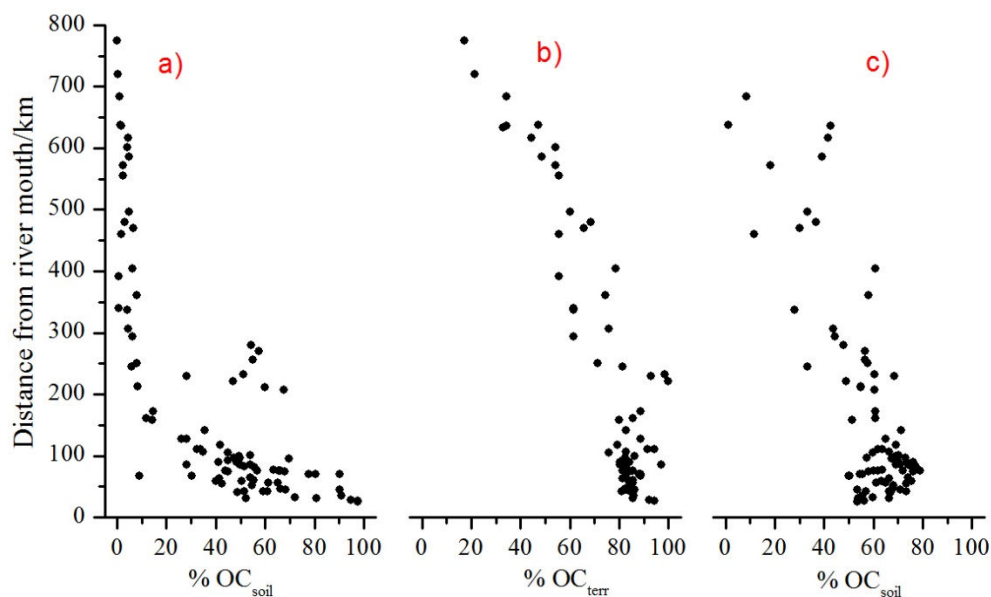
800   Table 1: Parameters including brGDGTs IIIa/IIa, Ia/IIa, the BIT index, MBT, MI, DC,

801   percentages of tetra-, penta- and hexa-methylated brGDGTs, and the weighted average

802   number of cyclopentane moieties (#rings for tetramethylated brGDGTs) based on the

803   GDGTs from three cores (M1, M3 and M7; see figure 2) in the Bohai Sea. Different

804   letters in parenthesis (a, b, c, d) represent significant difference at the level of $p<0.05$.

Indexes	Soil	M1	M3	M7
IIIa/IIa	0.39±0.25 (a)	0.63±0.06 (b)	1.16±0.12 (c)	0.93±0.07 (d)
Ia/IIa	4.93±9.60 (a)	0.59±0.07 (b)	0.81±0.06 (b)	0.91±0.05 (b)
BIT	0.75±0.22 (a)	0.50±0.19 (b)	0.14±0.06 (c)	0.11±0.03 (c)
MBT	0.45±0.30 (a)	0.32±0.03 (b)	0.33±0.01 (b)	0.38±0.01 (ab)
MI	4.70±0.42 (a)	4.88±0.05 (b)	4.91±0.03 (b)	4.81±0.02 (ab)
DC	0.31±0.21 (a)	0.62±0.03 (b)	0.79±0.03 (c)	0.82±0.02 (c)
%tetra	0.45±0.30 (a)	0.32±0.03 (b)	0.33±0.01 (c)	0.38±0.01 (c)
%hexa	0.16±0.12 (a)	0.20±0.02 (b)	0.24±0.02 (b)	0.20±0.01 (b)
%penta	0.39±0.20 (a)	0.48±0.02 (b)	0.44±0.02 (b)	0.42±0.01 (b)
#Rings$_{tera}$	0.20±0.15 (a)	0.39±0.03 (b)	0.47±0.02 (c)	0.47±0.02 (c)

805

806